NRC Research Press

ARTICLE

Pedunculate oak decline in southern Belgium: a long-term process highlighting the complex interplay among drought, winter frost, biotic attacks, and masting

Julie Losseau, Mathieu Jonard, and Caroline Vincke

Abstract: Since 2013, pedunculate oak (*Quercus robur* L.) mortality has been observed in the Ardennes region of Belgium. We aimed to understand the current decline by retrospectively (1945–2015) studying radial growth patterns of trees classified by three health statuses (reference, declining, and dying) and by linking them to abiotic and biotic hazard history, which we recorded and quantified. Our results show that oak mortality in the Ardennes is a long-term process, with 1987 as a tipping point for growth trajectories of declining and dying trees. That year was preceded by two growth crises (1976–1981 and 1984–1987), and it falls within the last major episode of oak decline in Belgium. Among hazards, very cold winters and caterpillar outbreaks have significant impacts on growth-pattern differentiation. Apart from 1976, extreme drought is still rare; however, mild spring droughts, especially in the years $n-1$ and $n-2$, explain some of the growth loss relative to the reference trees. Finally, masting appears to be an important contributing factor for the death of weakened trees. Given the direct and delayed impacts of the extreme drought of 1976 and subsequent water balance impairment due to winter frosts and mild spring droughts, the health of pedunculate oak is giving cause for concern in the context of climate change.

Key words: dendrochronology, forest decline, *Quercus robur* L., biotic and climatic hazards, mortality process.

Résumé : La mortalité du chêne pédonculé (*Quercus robur* L.) est observée depuis 2013 dans la région des Ardennes en Belgique. Nous avons cherché à comprendre la cause du dépérissement actuel en étudiant rétrospectivement (1945–2015) les courbes de croissance radiale des arbres classés selon leur état de santé (témoin, dépérissant et mourant) et en les reliant aux aléas biotiques et abiotiques passés que nous avons notés et quantifiés. Nos résultats montrent que la mortalité du chêne dans les Ardennes est un processus à long terme et que 1987 est un point tournant dans les trajectoires de croissance des arbres dépérissants et mourants. Cette année a été précédée par deux crises de croissance (1976–1981 et 1984–1987) et cela correspond au dernier épisode majeur de dépérissement du chêne en Belgique. Parmi les aléas, des hivers très froids et des épidémies de chenilles ont des impacts significatifs sur la différentiation des courbes de croissance. À l'exception de 1976, la sécheresse extrême est encore rare; cependant, de légères sécheresses printanières, particulièrement lors des années $n-1$ et $n-2$ expliquent une partie de la perte de croissance relativement aux arbres témoins. Finalement, la production massive de semences semble être un facteur qui contribue de façon importante à la mort des arbres affaiblis. Étant donné les impacts directs et à retardement de la sécheresse extrême de 1976 et la perturbation subséquente de l'équilibre hydrique à cause des gels hivernaux et des légères sécheresses printanières, l'état de santé du chêne pédonculé est une source de préoccupation dans le contexte du changement climatique. [Traduit par la Rédaction]

Mots-clés : dendrochronologie, dépérissement des forêts, *Quercus robur* L., aléas biotiques et climatiques, processus de mortalité.

1. Introduction

Several pedunculate oak (*Quercus robur* L.) decline crises were recorded and studied in Europe over the course of the 20th century (Delatour 1983; Haavik et al. 2015). The three major waves of oak decline observed in Belgium illustrate this European phenomenon well: the first crisis took place at the beginning of the 20th century (1911 and 1921–1923); the second occurred between 1941 and 1943; and the third occurred between 1983 and 1987, with a mortality peak in 1987 (Focant and Malaisse 2001). Since this last period, the phenomenon has never completely disappeared in some locations. In 2014, an upsurge of mortality was observed in several stands, mainly in the first foothills of the Ardennes in Belgium (Fig. 1). The process mainly affected large pedunculate oak trees (diameter at breast height (DBH; breast height = 1.30 m) > 30 cm). As this species is an economically and ecologically important deciduous forest tree species in Europe, these episodes of decline give cause for concern.

The theories explaining episodes of tree decline involve a complicated and poorly understood group of abiotic and biotic agents that reduce tree growth and vigor, degrade foliage and root systems, and ultimately cause tree mortality (Landman 1994; Haavik et al. 2015). However, it is generally accepted that three sets of factors are successively involved and progressively affect tree vitality (Manion 1991). First, predisposing factors acting over long time periods put permanent stress on trees and render them vulnerable; site conditions (such as hydromorphic soil) and past stand history are examples of such factors. Second, inciting factors, also called hazards, are of short duration but high intensity and may cause severe injury; these include winter frost (Hartmann and Blank 1992), spring or summer drought (Andersson et al. 2011), and defoliators (Bréda and Badeau 2008). Third, contributory factors

Received 8 October 2019. Accepted 18 December 2019.

J. Losseau, M. Jonard, and C. Vincke. Earth and Life Institute, Université catholique de Louvain, Croix du Sud, 2 L7.05.09, Louvain-la-Neuve, Belgium.
Corresponding author: Caroline Vincke (email: caroline.vincke@uclouvain.be).

Fig. 1. Location of the study sites and the declining stands reported to the Walloon Forest Health Observatory (OWSF) during the summer of 2014. B, Basse-Bodeux; D, Devantave; L, Louette-Saint-Pierre; R, Rienne. The map was created using ArcGIS software (10.6) by Esri and assembled from the following data sources: surveyed declining stands (OWSF 2014) and studied sites (personal field data). Base map from http://thematicmapping.org/ (provided by Bjorn Sandvi, from public domain sources). Photograph courtesy of OWSF. [Color online.]

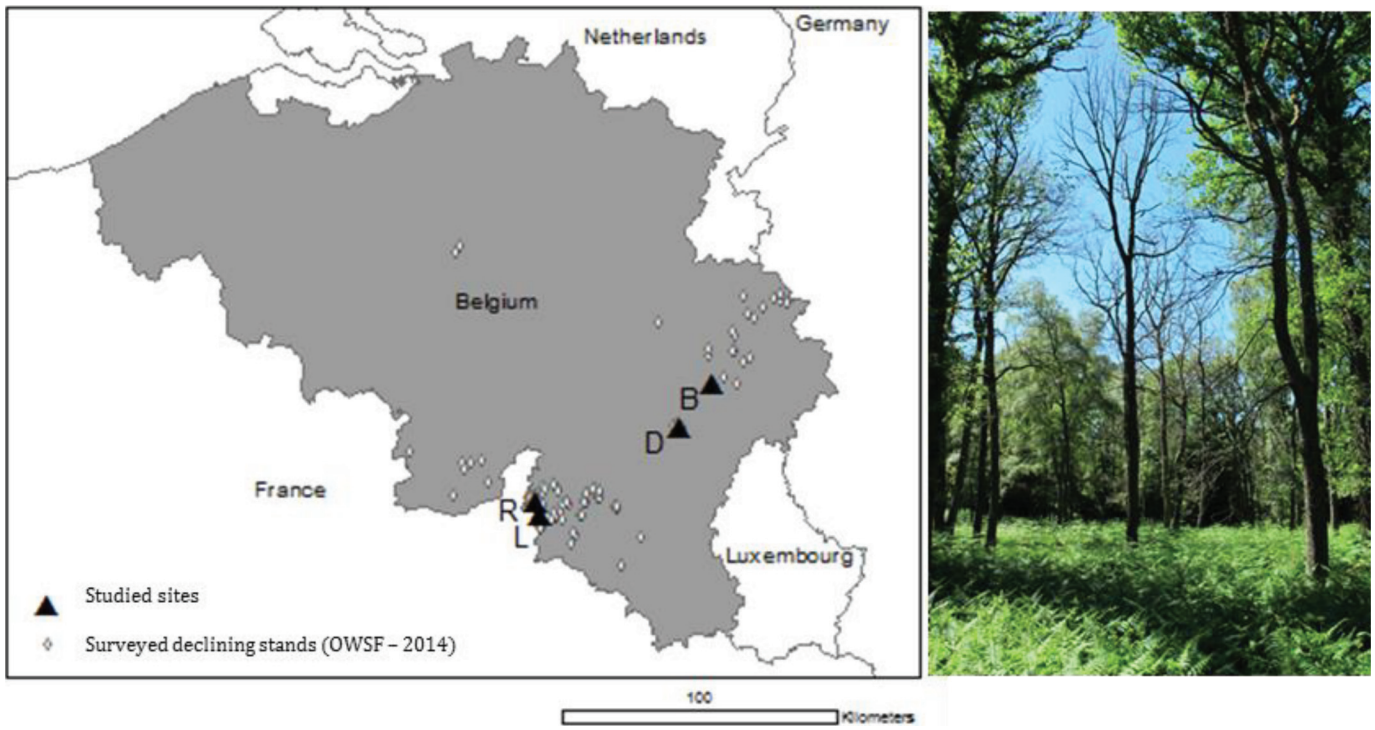

such as *Agrilus biguttatus* (Fabricius, 1777) (Hartmann and Blank 1992) or species of *Armillaria* (Fr.) Staude (Denman et al. 2017) can cause the death of declining trees. The length of time between the occurrence of two hazards, the intensity of hazards, and the phenological stage of the trees when the hazards occur are essential factors in potential recovery or decline (Bréda and Peiffer 2014). The literature highlights the increased frequency of extreme climatic events that have potentially dramatic impacts, both immediate and delayed, on tree and forest health (Bréda et al. 2006; Niinemets 2010; Allen et al. 2015; Rodríguez-Calcerrada et al. 2017). Interactions that may occur among abiotic and biotic hazards also complicate the decline analysis. For example, a defoliator outbreak renders oaks more susceptible to climate extremes such as drought and frost (Thomas et al. 2002). Furthermore, summer drought can make trees more sensitive to winter and spring frost through a decrease in photosynthate and nonstructural carbohydrate (NSC) reserves (Thomas et al. 2002).

The key physiological mechanisms underlying decline and tree mortality are still a matter of study and debate (McDowell 2011; Anderegg et al. 2012; Sala et al. 2012; Hartmann et al. 2018), with a particular emphasis on the fundamental interdependencies between carbohydrate metabolism and tree hydraulics. The first mechanism is carbon starvation, often associated with long-term growth decline before the mortality event (McDowell 2011), during which a tree's long-term carbon balance is in deficit, with consequent impacts on growth, maintenance processes, resistance to pathogens or insects, and embolism repair potential (Sala et al. 2012), sometimes leading to death. The second mechanism is hydraulic failure, which is associated with catastrophic xylem embolism following intense drought, leading to interruption of water transport. Ultimately, the two mechanisms are physiologically interlinked through their impacts on the integrity of the long-distance transport and coordination of the vascular system (Anderegg et al. 2012), which play an essential role in enhancing stress resistance in the long term (Sala et al. 2012).

As climate change is already triggering tree mortality around the world (Allen et al. 2015), the need to assess forests' capacity to cope with extreme events and the need to predict future mortality are stressed. However, as the factors involved last for different periods of time and interact at different stages of stand development, it is difficult to identify which factors initiate or accelerate the process of tree decline and mortality (Haavik et al. 2015). In addition, the duration of the decline or mortality process is highly variable and can extend over several decades and be expressed through different growth patterns (Camarero et al. 2015; Cailleret et al. 2017). Knowledge of abiotic and biotic hazard history (year, order, and intensity) and the development of tools that enable an understanding of past growth are therefore crucial. Past abiotic hazards have been widely studied, as climatic data sets over long time periods are available for many regions. However, past biotic attacks and mast events are often missing, which impedes a long-term systemic approach.

The Belgian Ardennes is a region with 57.2% forest cover. Norway spruce (*Picea abies* (L.) Karst.), European beech (*Fagus sylvatica* L.), and oak species (pedunculate oak and sessile oak (*Quercus petraea* (Matt.) Liebl.)) represent 43.6%, 16.6%, and 14.8% of the forest cover, respectively. In this region, even though the pedunculate oak is within its main ecological range in the temperate oceanic climate in the foothill zone, severe pedunculate oak decline and mortality were observed in 2014 (Losseau et al. 2018), covering a minimum of 1000 ha with up to 80% pedunculate oak mortality. In this study, we aimed to understand the current pedunculate oak decline process in the Ardennes. First, we retrospectively studied radial growth patterns (over the period of 1945–2015) of pedunculate oak trees of contrasting health status in terms of their level of crown defoliation in 2014 to investigate when and how patterns diverged. The trees were from four different sites, but we merged the chronologies of the four sites according to health status. As the decline and mortality observed in

Table 1. Characteristics of the four selected sites in terms of localization, stand characteristics, soil properties, and climate.

Characteristic	Rienne	Louette-Saint-Pierre	Devantave	Basse-Bodeux
Localization and topography				
Coordinates	49.9840°N, 4.8644°E	49.9382°N, 4.8878°E	50.2223°N, 5.5993°E	50.3612°N, 5.7695°E
Elevation (m a.s.l.)	375	390	500	450
Slope	<10%	<10%	<10%	<10%
Stand characteristics				
Oak age (years)	87 (13.4)	109 (2.2)	100 (15.9)	91 (25.9)
Oak GBH (cm)	120 (27)	152 (23)	114 (18)	99 (38)
Oak height (m)	27 (3)	26 (2)	23 (3)	23 (4)
Oak basal area ($m^2 \cdot ha^{-1}$)	14.9	15.6	12.6	16
Stand basal area ($m^2 \cdot ha^{-1}$)	17.8	26.6	12.6	24.4
Oak mortality	15%	32%	28%	43%
Last thinning	2009	2010	2012?	2010
Soil properties				
pH of soil water	4.4	4.2	4.5	4.4
Soil depth (cm)	100	120	100	140
SEW (mm)	130	160	60	111
Annual climate (1954–2015)				
Precipitation (mm)	1219 (207)	1219 (207)	972 (158)	1144 (185)
Mean temperature (°C)	8.21 (0.77)	8.21 (0.77)	8.26 (0.71)	8.26 (0.82)
Climate for the vegetation period (between 1 April and 31 October in 1954–2015)				
P-PET (mm)	12 (172)	12 (172)	−25 (152)	44 (164)

Note: Values in parentheses denote standard deviation. Coordinate system: Belge Lambert 72. a.s.l., above sea level; GBH, girth at breast height (breast height = 1.30 m); SEW, soil extractable water; P-PET, difference between precipitation (P) and potential evapotranspiration (PET).

2013–2014 were Ardennes-wide, we hypothesized that there would be a common trend despite local site differences. We also hypothesized that recent oak decline in the Ardennes is a long-term process and that the decline in growth of the trees that died in 2014 started before that of the declining trees. Second, we recorded past biotic and abiotic hazards over the period of 1955–2015 (for which we have meteorological data), quantified their intensity when possible, and related them to radial growth. The objective here was to assess which hazard association affects tree vitality. In the discussion, we try to relate our results to the theoretical framework of tree mortality described by McDowell (2011), taking into account the interdependencies between the two main mechanisms of carbon starvation and hydraulic failure.

2. Materials and methods

2.1. Sites

In 2015, four sites exhibiting pedunculate oak mortality were selected in two subregions of the Belgian Ardennes. Two sites, Rienne and Louette-Saint-Pierre, are located in the Basse and Moyenne Ardenne, and the other two sites, Devantave and Basse-Bodeux, are in the Ardenne Centro-Orientale (Fig. 1). According to a survey carried out by the Walloon Forest Health Observatory (OWSF) in 2014, most of the reported sites with declining pedunculate oaks are in these two regions (OWSF 2014). These regions present higher annual precipitation rates and lower annual mean temperatures than the rest of Belgium because of their higher elevations (Van der Perre et al. 2015). The selected sites contain mainly pedunculate oak, mixed with some sessile oak trees growing on acidic stony loam soils (Table 1).

2.2. Tree and stand measurements

2.2.1. Sampling design

At each site, a 0.5 ha rectangular plot was established in July 2015. Tree species and circumference at breast height were recorded for all trees above the inventory threshold (circumference > 40 cm) (Table 1). The two oak species (pedunculate oak and sessile oak) were identified with binoculars, based on acorn and leaf morphology in the upper crown. The total height of all the trees was measured to deduce dominant height. This was defined as the mean height of the largest 20% of living trees.

2.2.2. Dendrochronology

At each site, 24–28 dominant or codominant pedunculate oak trees were selected in August 2015. These two social status groups include trees with a height above the dominant height minus 2 m and a girth at breast height (GBH) above the mean GBH. Assessments of crown condition were carried out on the part of the crown free of competition from neighboring trees. The defoliation of the assessable crown was visually estimated on the basis of 5% classes by comparison with a local reference tree corresponding to the healthiest tree that was able to grow at a particular site (ICP Forests protocol; Eichhorn et al. 2016). We established three different health statuses for trees: reference, declining, and dying. Reference trees were the healthiest trees in 2015, with a mean defoliation of 20%; declining trees had a mean defoliation of 60% in 2015; and dying trees were trees that had died recently (100% defoliation), mostly in 2014 (Table 2).

Selected trees were sampled in October 2015 by extracting two perpendicular increment cores at breast height with a 5 mm Haglöf increment borer (Haglöf Sweden, Långsele, Sweden). Cores were mounted on wooden plates, and their surfaces were prepared using a microtome. The entire cores were scanned using a high-resolution, distortion-free digital scanner (Epson Expression 1000 XL, Seiko Epson Corporation, Suwa, Japan). Ring width, earlywood width, and latewood width chronologies were recorded using WinDENDRO (Regent Instruments Inc., Quebec, Que., Canada). They were visually cross-dated using skeleton plots and assessed using COFECHA (Grissino-Mayer 2001). As the death dates of the dying trees were unknown, all cores from dying trees were visually cross-dated and validated again using COFECHA once a reliable chronology had been developed with cores from reference and declining trees. For each tree, the two core measurements were averaged before chronologies were constructed at the stand or regional level. The period studied (1945–2015) was chosen to have a common interval for at least six trees per chronology (Mérian and Lebourgeois 2011). As we did not want to erase any

Table 2. Number of cored trees per health status for each stand.

Health status	No. of cored trees
Rienne	
Reference	8
Declining	7
Dying	10
Louette-Saint-Pierre	
Reference	8
Declining	10
Dying	10
Devantave	
Reference	6
Declining	8
Dying	10
Basse-Bodeux	
Reference	9
Declining	6
Dying	10

signal linked to the process of decline, no standardization procedure was used to compare growth patterns between tree species and health status.

The distinction between sapwood and heartwood was determined based on wood coloration and a contrast in tylose density. The oldest year in sapwood was identified, and sapwood length was deduced based on previous ring width measurements. Sapwood rings with earlywood vessels filled with tyloses were listed at tree level based on binocular observations. All earlywood vessels in sapwood that were filled with mycelium structure were also counted. The results are displayed in the Supplementary data.[1]

2.3. Characterization of factors affecting tree vitality

2.3.1. Climatic index

Data on daily precipitation and minimum and maximum daily temperatures were obtained from the Royal Meteorological Institute of Belgium (RMI) for each site for the period of 1954–2015. Data were extracted from a 10 km × 10 km grid-based database. Mean daily temperature was estimated by averaging the minimum and maximum daily temperatures. We calculated a winter index to detect winter frost stress as the sum of mean daily temperatures for the days with a mean temperature below 0 °C from 1 October to 1 April (Klap et al. 1997). All the years with –20 °C days were considered as extremely cold winters (Hendriks et al. 1997). Climatic drought events were investigated using the standardized precipitation evapotranspiration index (SPEI) (Vicente-Serrano et al. 2010), which combines precipitation and temperature data to calculate a climatic water balance. SPEI was calculated from May to July and from August to October to distinguish between spring and summer droughts, based on Hargreaves' potential evapotranspiration (PET) equation (Hargreaves and Samani 1985). This PET equation has the advantage of requiring few climate variables (observed minimum and maximum daily temperatures) and is therefore useful for PET calculation for periods during which climatological data are scarce.

2.3.2. Caterpillar outbreaks and massive masting events

Caterpillar outbreaks were listed at the regional level using the caterpillar attack records of the OWSF (2011–2015) and the ALEA database (Piraux et al. 2016), which lists all extreme events occurring in Belgium on the basis of literature (1893–2013) and previous studies of oak decline in Belgium. Caterpillars associated with outbreaks in Belgium include *Erannis defoliaria* (Clerck, 1759), *Operophtera brumata* (Linnaeus, 1758), and *Tortrix viridana* (Linnaeus, 1758), all of which develop in early spring. The ALEA database was also used to identify years of high acorn production. It was supplemented for 1995–2015 with data from the Seed Production Center (Comptoir Forestier). Acorn production is monitored each year in forest seed orchards, and years are classified as very good, good, medium, or poor. We retained only the first two classes, as we were interested in mast events that might affect tree carbon balance and tree health if associated with other biotic or climatic stresses.

2.4. Data analysis

Dendrochronological data were first analyzed at the regional level over the period of 1945–2015 by merging the chronologies of the four sites according to health status. We hypothesized that the tree decline and mortality observed in 2014 had been caused by the same drivers, as this phenomenon occurred simultaneously in various parts of the Ardennes region. To highlight this common pattern and improve the quality of the signal, we first averaged the chronologies to reduce the noise due to the site effects. From all the cored trees (Table 2), we selected the same numbers of pedunculate oak trees in each site and health status (reference, declining, and dying), ensuring balanced numbers and avoiding factor confusion between site and health status. We selected 27 trees per health status. Differences among health statuses were assessed at the year level using the Wilcoxon test ($\alpha = 0.05$), comparing declining and dying trees with the reference trees. For each year, and still at the regional level, we also calculated the relative growth loss (difference between the ring width of reference trees (RW_{ref}) and that of dying trees (RW_{dying}) or declining trees ($RW_{declining}$) in relation to the reference ring width; eq. 1):

$$\text{(1)} \qquad \text{Relative growth loss} = (RW_{ref} - RW_{dying} \text{ or } RW_{declining})/RW_{ref}$$

By calculating the difference between the ring width of reference trees and that of declining or dying trees, we removed the effects of the drivers affecting the growth of the various tree statuses equally and highlighted the years for which the growth dynamics of declining or dying trees differed from that of reference trees. Standardizing this difference based on the ring width of reference trees allowed comparison of sites regardless of growing conditions. To describe the temporal pattern of the relative growth loss and identify the onset of tree decline, we used a segmented regression to account for the fact that relative growth loss remained comparatively limited until 1987, from which point it steadily increased.

In addition to relative growth loss, we used three other indices to describe the immediate and delayed impacts of hazards on tree growth. First, we identified the "growth crisis" period for each group of trees. This is defined as a period during which annual growth of the group is lower than the reference pedunculate oak mean ring width for at least 3 years, calculated from 1945 to 2015 at the regional level. Second, to highlight the impact of specific hazards, we calculated regional pointer years (PYs; Schweingruber 1996), which are defined as those calendar years in which at least 75% of the cross-dated trees present an absolute value of radial growth variation higher than 10% of their individual growth the preceding year (Becker and Lévy 1990), whether increasing (positive PY) or decreasing (negative PY). Third, the latewood percentage (LW%) at ring level was computed because a lowered LW% is

[1]Supplementary data are available with the article through the journal Web site at http://nrcresearchpress.com/doi/suppl/10.1139/cjfr-2019-0341.

Fig. 2. Mean tree-ring series at the regional level for reference, declining, and dying trees (number of cored trees = 27). Trees were balanced at the stand level. Differences between declining and dying trees versus reference trees at the year level were tested using the Wilcoxon test at a significance level of 0.05. Asterisks (*) denote declining trees, and black squares (■) denote dying trees.

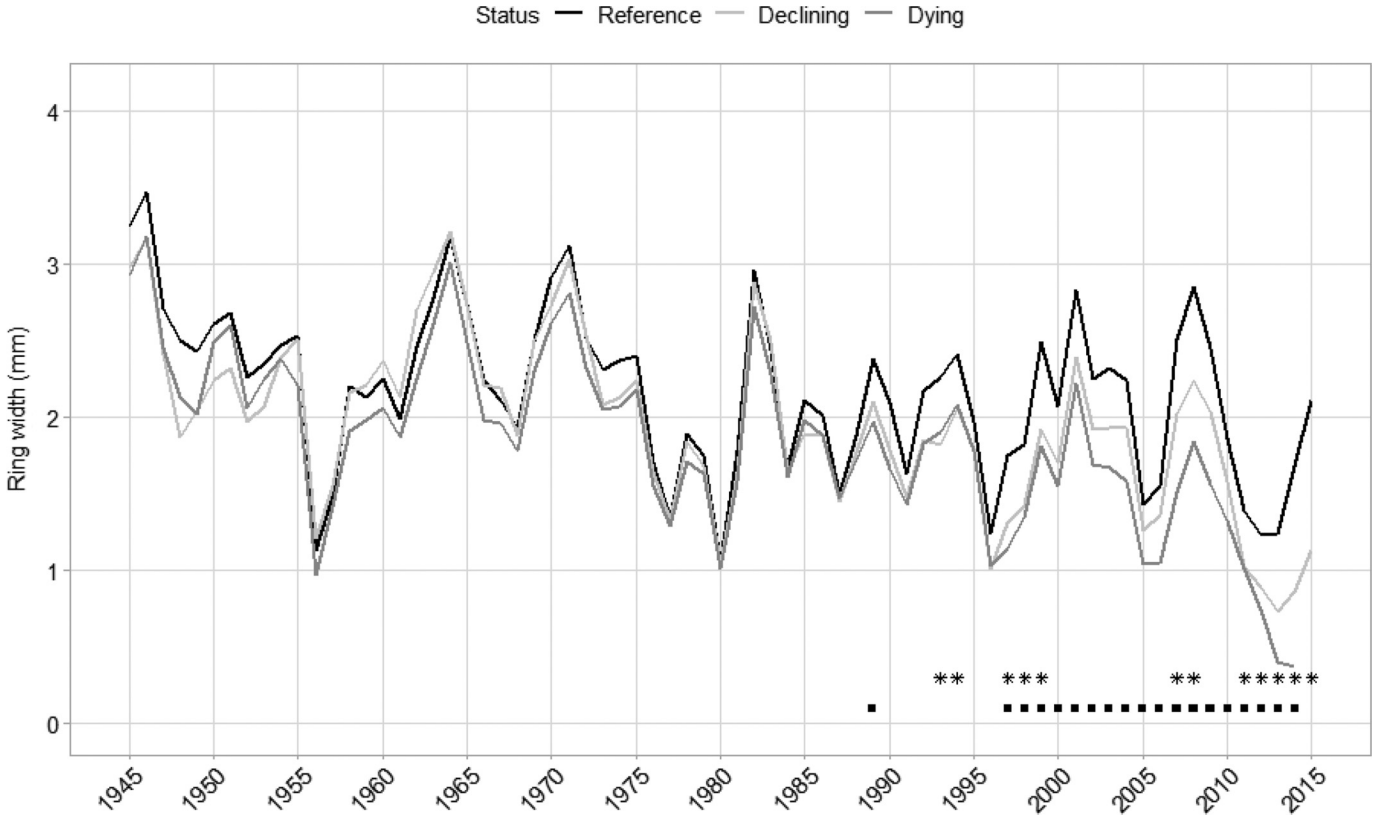

related to a decline trajectory (Rubtsov 1996); we listed years with LW contributing to less than 60% of ring width, which is the long-term mean of LW% for reference trees.

In addition, ring width chronologies were constructed at stand level by averaging tree data (Table 2), and the relative growth loss was calculated for the various health statuses. To identify which factors best explained the radial growth loss of declining and dying trees, we developed multivariate linear models using the stepwise procedure of variable selection (forward) based on the Bayesian information criterion (BIC). The factors considered in this analysis were winter index, caterpillar outbreaks, and masting events of the current year (n) and spring (May–July) and late summer (August–October) SPEI of the current year (n) and the two preceding years ($n - 1$ and $n - 2$). The site effect was also incorporated into the analysis, as the sequence of hazards was different among sites. We considered only the period of 1987–2015 because radial growth loss was very limited before 1987. For dying trees, a multivariate model was also applied for the period of 2010–2015, during which radial growth loss strongly increased. The normality of the residuals was checked using Q–Q plots and normality tests.

All statistical analyses were carried out using R (R Core Team 2013) and JMP Pro 14.1.0 (SAS Institute, Cary, N.C., USA).

3. Results

3.1. Comparison of health statuses at the regional level

Declining trees had an annual radial growth that differed from that of the reference trees between 1993 and 1999 ($p < 0.05$) and between 2007 and 2015 (Fig. 2). Dying trees had significantly lower growth from 1997 up to death (Fig. 2; $p < 0.05$). From 1987 to 2015, the difference in growth between reference and dying trees was significant ($p = 0.0005$), as was the difference between reference and declining trees ($p = 0.0128$), but no significant difference was observed between declining and dying trees ($p = 0.5490$). Thus, growth decline seems to have started around 1987 for the declining trees, as after this year, growth never reached the level of reference trees again. Radial growth of dying trees was below even that of reference trees since 1945, although between 1975 and 1984 (a period with severe droughts like in 1976 and 1983), they both had the same annual growth. The segmented regression (Fig. 3) showed that declining and dying trees had a slightly lower radial growth than reference trees until 1987 (–6%) and then started to progressively deteriorate to reach 40% relative growth loss in 2015.

Fig. 3. Temporal trend in relative growth loss of declining or dying pedunculate oak trees compared with reference trees (eq. 1). We highlighted pattern shifts around 1987 by applying a segmented regression to the data (dashed line). R^2, coefficient of determination.

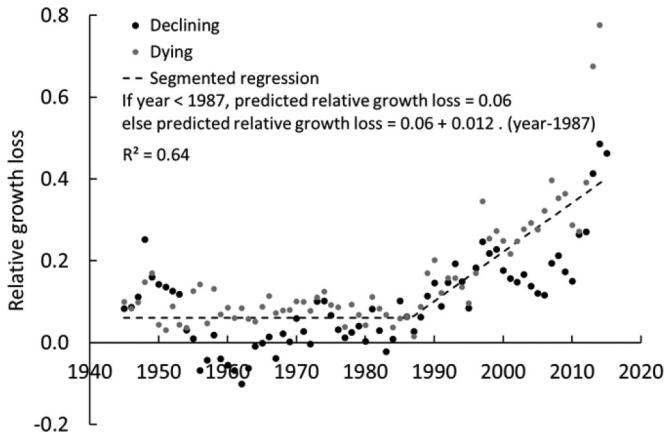

Fig. 4. Sapwood proportion according to health status at regional level. Differences among health statuses were assessed via an analysis of variance (ANOVA) followed by a post hoc Tukey's test. Groups A and B are significantly different at a significance level of 0.05.

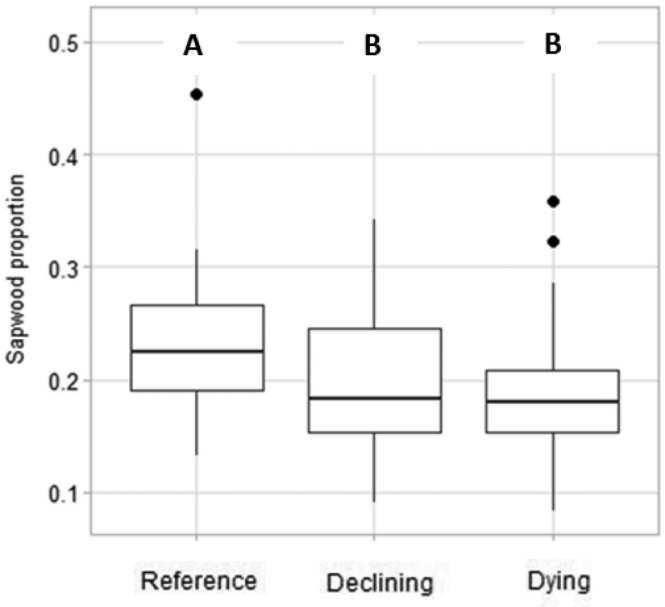

Sapwood proportion ranged from 18% to 23% of the total radius (Fig. 4), with the lowest values for the dying and declining trees, which were significantly different from those of the reference trees.

LW% did not differ significantly among health statuses (data not shown) until 2012, with a maximum of 70% when ring width was greater than 2.5 mm, a long-term mean of 60%, and a minimum of 2% in the year prior to death.

In over 80% of dying tree cores, mycelium structures were found in the sapwood, together with tyloses, which sometimes filled all earlywood vessels (Supplementary Fig. S1[1]).

3.2. Factors involved in the decline process

Mean ring width of the reference trees was 2.13 mm (standard deviation = 0.53), and this was the baseline used to define the "growth crisis" for health status (i.e., a period during which radial growth was below this value for at least three successive years) (Fig. 5). For reference trees, a first growth crisis took place in the period of 1956–1959, followed by a second growth crisis in 1976–1981, a third growth crisis in 1984–1988, a fourth growth crisis in 1995–1998, and a fifth growth crisis that started in 2010 and had not yet ended in 2015. The first two growth crises impacted tree growth independently of defoliation status in 2015 (although dying trees experienced an additional small growth crisis in 1966–1968). However, following the third growth crisis (1984–1988), declining and dying trees experienced a continuous decline in growth, which led to a growth crisis that persisted until 2015. Following three successive years of caterpillar outbreaks (2011–2013) and a powdery mildew attack in 2012–2013, a recovery in growth was observed only in reference and declining trees.

In the period of 1955–2015, eight negative PYs were common to the three chronologies over the whole region (one between 1955 and 1975 and seven between 1976 and 2015), indicating strong environmental constraints on radial growth by comparison with the preceding year. Most of the time, the LW% fell below 60% of ring width for the same year. For the declining and dying trees, the frequency of years with a low LW% has increased over time since the beginning of the 1990s.

Six extreme winters were associated with negative PYs (with 1956 leading to a growth reduction of more than 50%), and four extreme winters were associated with low LW% (1956, 1986, 1987, and, to a lesser extent, 2010) or more generally with the beginning of a growth crisis (Fig. 5). Three consecutive extreme winters occurred in 1985, 1986, and 1987, in the middle of the third growth crisis, after which the growth of declining and dying trees diverged from the reference growth.

Since 1955, climatic drought has been observed 11 times in spring and early summer and 13 times in late summer and early autumn, with some episodes lasting the whole growing season (1959, 1975, and 1976). The longest growth crisis for the reference trees started with the droughts of the early 1970s (1973 and 1975) and especially the drought of 1976, which was the most intense of the chronology (in terms of precocity, duration, and water deficit), reinforced by the droughts of 1983 and 1985. Mild drought events also impacted trees, with observable effects that were often delayed and cumulative. We observed that five out of seven particularly negative PYs (1956, 1976, 1980, 1987, 1996, 2005, and 2011) were preceded by one or two droughts.

Massive (regional-scale) mast events have been recorded 12 times since 1955, some of them following droughts (1976, 1995, 1998, 2000, 2004, and 2006). Known intense caterpillar outbreaks (1980, 1996, 2005, and 2011–2013) were associated with significant growth decrease in the same year (negative PYs and low LW%). Two of the caterpillar outbreaks occurred at the beginning of a growth crisis (1996 and 2011), and the mortality event of 2014 followed three consecutive years of major caterpillar attacks.

To perform statistical analysis of the effects of abiotic and biotic hazards, we pooled both declining and dying statuses and all sites for the period of 1987–2015 and looked at the drivers of the relative growth loss (eq. 1) using a variable selection procedure (Table 3, upper panel). The growth loss of declining and dying trees relative to reference trees amounted to, on average, 22.3% and increased significantly with the winter index. When a caterpillar outbreak occurred, the relative growth loss was higher than that of years without a caterpillar outbreak (+5.3%). Spring drought during the current year (n) and the two preceding years ($n-1$ and $n-2$) reinforced the relative growth loss as shown by the negative effect of the May–July SPEI. In contrast, the August–October SPEI of the two preceding years ($n-1$ and $n-2$) had a significant impact on the relative growth loss, meaning that rainy conditions in late summer tended to increase the relative growth loss of declining and dying trees as compared with reference trees. Finally, the relative growth loss was higher in Basse-Bodeux and Louette-Saint-Pierre than in Devantave, which is the site with the lowest soil extractable water (SEW; Table 1). All of these factors explained 32% of the variability. When focusing only on dying trees and on the period during which mortality was observed (Table 3, lower panel), the relative growth loss was higher (33.84%) and increased in the year with the massive masting event (+11.2%). SPEI effects were detected only for the year $n-2$, with a negative impact of the May–July SPEI (spring drought enhancing relative growth loss) and a positive impact of the August–October SPEI (rainy conditions favoring relative growth loss). This second multivariate model explained 87% of the variability.

4. Discussion

4.1. Growth-pattern characterization and mechanisms at play

The trees analyzed in this study were differentiated according to their health status in 2015, with the level of defoliation used as a proxy for tree vitality. Defoliation class proved to be a very useful integrative indicator of life trajectories of trees in a long-term perspective. Looking at their growth rings and taking into account the critical transition in 1987 (Fig. 3), we showed that the decline process started at least 28 years before the upsurge of

Fig. 5. (*a*) Radial growth for reference, declining, and dying pedunculate oak trees at the regional level. The dashed horizontal line represents the mean ring width for reference pedunculate oak over the period of 1945–2015. Shaded areas below this line correspond to growth crisis periods. (*b*) Pointer years (PYs), latewood percentage (LW%), and past stress encountered over the period of 1954–2015. Positive PYs are in grey, and negative PYs are in black. Years with LW% less than 60% of ring width are in black. For the winter index, black cells indicate the coldest 10% of winters and grey cells indicate the warmest 10% of winters. For the standardized precipitation evapotranspiration index (SPEI; 3 months in May–July and August–October), values below –1 are in black (drought) and values above +1 are in grey (wet conditions). Mast years and caterpillar outbreak occurrences are indicated by black squares. Slashes indicate that no data are available because the trees died in 2014.

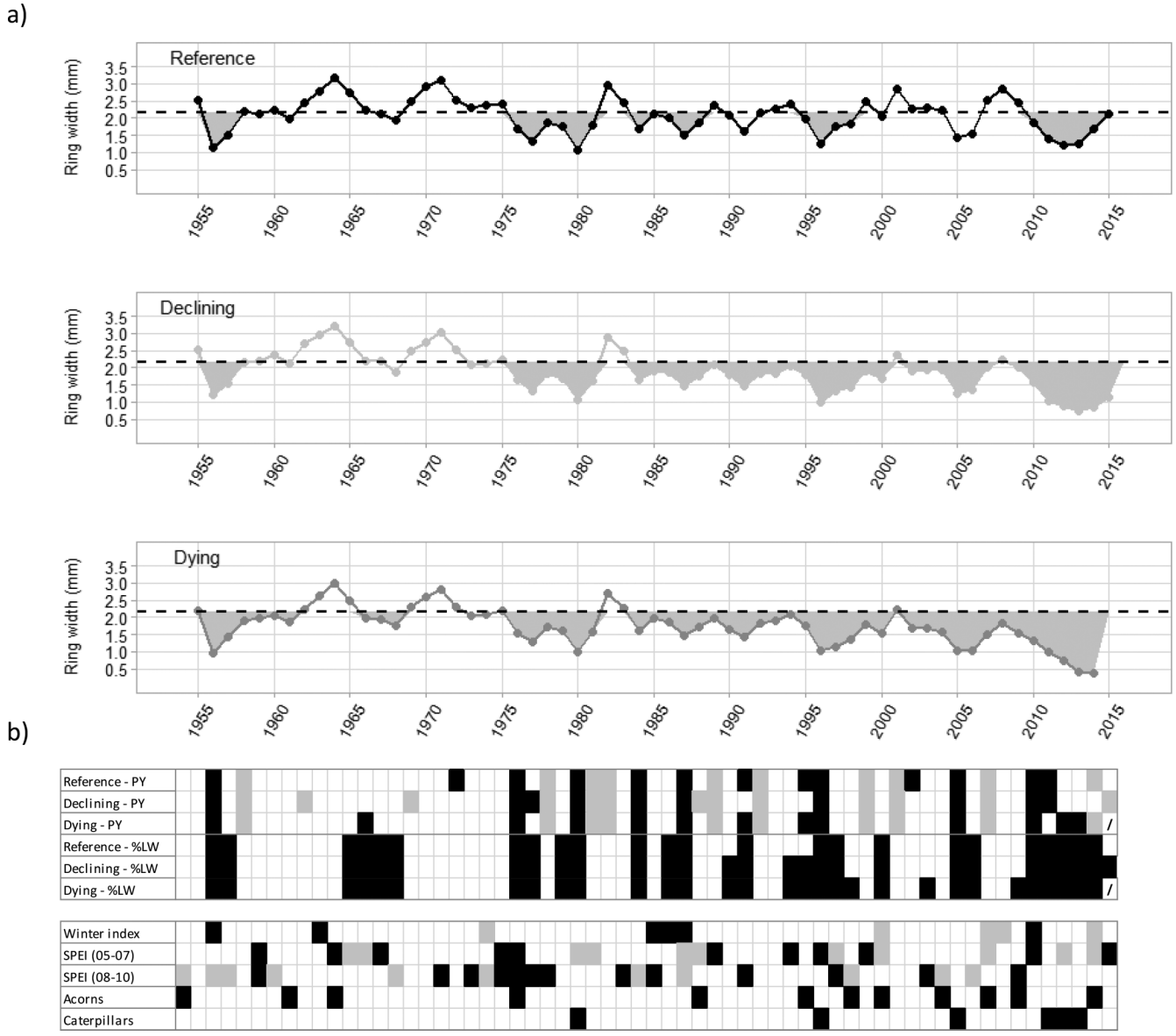

mortality in 2014 for all sites. Tree decline is commonly observed as a long-term process (Cailleret et al. 2017), with some exceptions; for example, tree decline can occur according to tree regeneration origin (Zadworny et al. 2019). The transition year of 1987 was also associated with high oak mortality throughout Belgium (Focant and Malaisse 2001). That year, which was identified as a tipping point for both declining and dying trees, led to an increase in the growth variability of the trees. In contrast to studies observing that high growth rates in the past may predispose trees to drought-related death (Voltas et al. 2013), dying trees in this study had already been growing less vigorously than the rest of the stand since the 1940s. The trees that we studied, including those that died in 2014, are the long-term survivors of past stresses and were therefore the most resilient trees of the original stand. As expected, the decline process that had been visible in radial growth since 1987 was more pronounced in dying trees than in declining trees. Divergences in patterns became even clearer after 2010, during the fifth growth crisis, when the growth of dying trees dropped dramatically; insect outbreaks (2010–2013) and mildew infection were the ultimate associated mortality factors, as also observed by Andersson et al. (2011). Furthermore, after 2011, dying trees produced only earlywood. As oak earlywood is produced before budburst (Sass-Klaassen et al. 2011), oak trees rely solely on NSC reserves from the previous growing season (Barbaroux and Bréda 2002) to build new vessels. This suggests that dying trees probably had just enough carbon to partly refill the NSC reserve to maintain the integrity of the hydraulic transport system (Sala et al. 2012) but were no longer in a position to produce latewood, especially when a caterpillar attack occurred in spring and early summer. This carbon starvation mechanism is

Table 3. Multivariate linear models explaining relative growth loss in declining and dying trees on the basis of the winter index, the occurrence of caterpillar outbreaks and mast events (binary response), the standardized precipitation evapotranspiration index (SPEI) calculated for May–July and August–October of the years $n-1$ and $n-2$ (Vicente-Serrano et al. 2010), and the site effect.

Effect	Estimate	SE	p value
1987–2015: declining and dying trees (R^2 = 0.32)			
Intercept (Rienne)	0.22324	0.02672	<0.001
Winter index	0.00064	0.00018	<0.001
Caterpillar outbreak [0, 1]	0.05274	0.01757	0.003
SPEI May–July	−0.05002	0.01242	<0.001
SPEI May–July ($n-1$)	−0.03273	0.01125	0.004
SPEI May–July ($n-2$)	−0.03242	0.01084	0.003
SPEI August–October ($n-1$)	0.03567	0.01379	0.010
SPEI August–October ($n-2$)	0.06549	0.01535	<0.001
Site (Basse-Bodeux)	0.04776	0.01760	0.007
Site (Devantave)	−0.05598	0.01743	0.002
Site (Louette-Saint-Pierre)	0.06627	0.01741	<0.001
2010–2015: dying trees (R^2 = 0.87)			
Intercept	0.33816	0.03735	<0.001
Mast event [0, 1]	0.11172	0.03895	0.011
SPEI May–July ($n-2$)	−0.11000	0.01757	<0.001
SPEI August–October ($n-2$)	0.18257	0.05216	0.003

Note: Models were obtained using the stepwise procedure of variable selection (forward) based on the Bayesian information criterion (BIC). SE, standard error; R^2, coefficient of determination.

often associated with long-term growth decline before the mortality event (McDowell 2011). In our case, hydraulic failure is not likely to be the single proximal cause of subsequent oak decline and mortality, as trees dying solely from hydraulic failure often do so quickly (Haavik et al. 2015).

In addition to differences in radial growth, we found that sapwood proportion was significantly greater for the reference trees than for others. This result is unsurprising, as the ring widths of declining and dying trees were also lower over the period during which sapwood was measured and sapwood proportion is also thought to be linked to levels of defoliation (Camarero et al. 2015). However, as a large part of NSC is stored in sapwood in proportion to the sapwood surface (Barbaroux and Bréda 2002), these results suggest that NSC reserves could have been lower in declining and dying trees, which therefore became caught in a vicious circle. Alternatively, this sapwood diminution could be seen to a certain extent as an acclimatization (Anfodillo et al. 2016): through defoliation and small-branch mortality, trees reduce their crown volume and water-conducting tissues to decrease their need for carbon for maintenance respiration. Nevertheless, this crown reduction also reduces carbon assimilation and thus reduces NSC.

4.2. Drivers of radial growth loss

As far as inciting factors of decline are concerned, an original feature of this work is our reconstruction of the regional history and intensity of recorded abiotic and biotic hazards over the past five decades. We were able to do this because the region is relatively small, with fairly uniform environmental conditions, and because of a developing interest in keeping archives about stand history. Our results confirm the significant role of (and complex interplay among) winter frosts, caterpillars, and drought (previous and current), as well as (more specifically for dying trees) the coincidence with massive masting and powdery mildew. We highlight the fact that it is necessary to have solid follow-up of hazards in forests (type, intensity, and frequency) and their impacts to be able to discuss mortality mechanisms.

Very cold winters have already been related to several cases of oak mortality (Thomas et al. 2002), and this is highlighted in the multivariate model (Table 3). In particular, the winters of 1985, 1986, and 1987 appear as inciting factors of oak decline in trees already weakened by a growth crisis triggered by an extreme drought (1976). Oaks have ring-porous wood, with large vessels in the earlywood contributing to the major part of water conduction. Large vessels are sensitive to embolism during winter, which is associated with the freeze–thaw cycle; partial embolism occurs each year in oaks during winter, as water freezes in vessels below −5 °C, so that water transport, relying mostly on the last ring, is jeopardized when winters are extremely cold (Ellmore and Ewers 1986; Granier et al. 1994). Furthermore, according to Thomas et al. (2002), necrosis develops in the root system and trunk during extremely cold winters. It affects bark, phloem, and cambium, hence affecting growth in the next growing season. It might be expected that spring frost would also have a strong impact, as it would affect vessels in formation and young leaves, but even though we found a significant positive relationship between May mean temperature and ring width, and earlywood and latewood indices (results not shown), no growth crisis or negative PY could be directly linked to severe spring frost.

Tree vitality is also affected by defoliation induced by caterpillar outbreaks, which leads to an increase in relative growth loss of declining and dying trees as compared with reference trees (Table 3). The known caterpillar outbreaks are probably the most intense and generalized ones because no systematic records were kept in southern Belgium before 2012. Thus, it is very likely that the impact of this hazard has been underestimated. Furthermore, its frequency seems to have increased over the last three decades. This may be due solely to better data archiving, but it may also be linked to the unbalanced foliar nutrition of oak induced by large, historical nitrogen deposition in the Ardennes (Jonard et al. 2012), which may have favored caterpillars. Caterpillars feed on leaves and therefore limit carbon assimilation. Vernal caterpillars affect carbon uptake in the short term and cannot alone cause tree death. Indeed, oaks have the capacity to produce new leaves in June (Thomas et al. 2002). Impacts will be much more dramatic if powdery mildew and (or) other caterpillar outbreaks follow the first caterpillars (Bréda and Badeau 2008; Marçais and Desprez-Loustau 2014). In Belgium, the death of weakened trees in 2014 was preceded by at least 3 years of caterpillar attacks, which were associated with powdery mildew in 2013.

The radial growth of the trees was similarly influenced by climatic variability regardless of crown conditions (correlations analysis; Supplementary Fig. S2[1]). Rainfall during autumn of the previous year and early spring of the current year, as well as favorable temperatures during May and July of the current year, is positively correlated with growth rates, as observed by Lebourgeois et al. (2004) and Andersson et al. (2011).

Pattern distinction relative to health status is also linked to delayed tree reaction to SPEI in two specific periods. The first period is May–July and relates to spring and early-summer drought from year $n-2$ to year n and more strongly affects declining and dying trees. The second period relates to the August–October SPEI of the two preceding years and shows that declining and dying trees do not benefit from the rainy conditions of late summer and the difference relative to declining or dying trees increases. This implies that declining and dying trees do not have the same ability as the reference trees to restore their carbon reserve after stress, which could be consistent with a carbon starvation mechanism and its subsequent consequences on whole-tree carbon dynamics, tree biotic interactions, and vascular system integrity (Hartmann et al. 2018).

As far as drought and its impacts are concerned, extreme droughts such as that of 1976 (which started very early in spring and followed a dry winter) are still statistically rare events in our chronologies. We therefore hypothesized that hydraulic failure processes associated with drought must be uncommon in the Ardennes. Some of the trees that experienced the severe drought

stress in 1976 (with very low LW% in 1977) were probably subsequently more vulnerable and could have had higher mortality rates or probability of decline in the event of a second drought or extreme hazard such as the 1983–1984 droughts followed by the winters of 1985–1987 (Bréda et al. 2006; Miao et al. 2009). Nevertheless, the multivariate linear models explaining relative growth loss showed the negative impacts of milder spring droughts, with legacy effects from years $n-1$ and $n-2$. These legacy effects may also be linked to the interplay between drought and caterpillars. Indeed, a mild drought can lead to a decrease in the ratio of carbon to nitrogen in the following year and make leaves more attractive to caterpillars (Rouault et al. 2006). Drought can also directly affect the pathogen cycle. For example, dry and warm summers reduce the larval period of *Lymantria dispar* (Linnaeus, 1758), which is favorable for causing outbreaks in the following year (Villemant and Fraval 1998). This may partially explain why we found that caterpillar outbreaks followed 1 or 2 years of spring or summer drought, as well as why we so often observe delayed effects of drought. These legacy effects give rise to particular concern in the current context of climate change, with an increase in spring drought coupled with a more precocious phenology.

Mast events also affect carbon balance. Masting is characterized by high interannual variability and a high level of synchronization in seed production at the population and community levels (Fernández-Martínez et al. 2012). In our case, half of the observed mast events were recorded following droughts, and the massive masting in 2014 was concomitant to mortality. During a mast year, ring width is known to be thinner (Sonesson and Drobyshev 2010) and carbon reserves are depleted. Thus, drought together with mast events and caterpillar outbreaks may negatively affect trees' carbon status.

Nutritional disorder was not studied because it is not a hazard per se but rather a press disturbance acting as a predisposing factor; however, it may play a part in the process of decline, as forest soils in the Ardennes are known to be poor and subject to a long history of high nitrogen atmospheric deposition (Jonard et al. 2012), which generates nutrient imbalances, especially with phosphorus, magnesium, and potassium. Lucassen et al. (2014) ascribed the decline in oak vitality in the north of Belgium to nutrient deficiencies, which were also suggested as a predisposing factor by Andersson et al. (2011). In addition, water stress can increase nutritional disorders (Kreuzwieser and Gessler 2010).

Finally, the vascular mycosis observed could be considered as a contributory factor, as it has already been associated with oak decline, especially with species of *Ophiostoma* Syd. & P. Syd. in Eastern Europe (Delatour 1983). *Verticillium* (Nees, 1816) mycosis was also observed in Belgium at the end of the 1980s in severely declining oaks (Galoux and Dutrecq 1990). We hypothesize that the observed mycelium structures developed in vessels when trees were still alive, as we also found tyloses in the last rings of recently dying trees. Tyloses are a defense mechanism and can be produced in reaction to fungal infections (De Micco et al. 2016).

5. Conclusion: global understanding of decline and the mortality process

Pedunculate oak decline and mortality observed in Belgium in 2014 are associated with a long-term process that began in the mid-1980s (at the earliest). It was provoked by a combination of stresses and their nonlinear interactions, which highlights the role of stress history (type of stress and order of event) in oak decline and mortality and the need to use a wide time perspective when analyzing factors that cause tree decline (Andersson et al. 2011). Associated hazards had already caused high mortality rates among pedunculate oaks at the end of the 1980s (André and Laudelout 1992), and the trees studied are those that were resilient at that time. After 1987, relative growth loss of declining and dying trees increased with time. This process worsened for dying trees after 2010. Dying and declining trees have been experiencing a continuous growth crisis since 1987, relative to the reference trees. Several hazards were identified as affecting tree vitality (Table 3). Severe winters led to several growth crises and affected growth during the following season, as did mild spring droughts. Defoliator outbreaks (whether preceded by drought or not) affected tree vitality, with masting and powdery mildew as contributory factors of mortality. This succession of hazards probably depletes NSC storage and has already been associated with oak mortality. The decline and mortality patterns and mechanisms described herein can be considered representative of other cases of pedunculate oak decline in the temperate oceanic climate in the foothill zone. Given the direct and delayed impacts of the extreme drought of 1976 and subsequent water balance impairment due to winter frosts, mild spring droughts, and transport system failure, the health of pedunculate oak is giving cause for concern in the context of climate change, as extreme climatic events are expected to increase in intensity and frequency.

Acknowledgements

Field measurements and core processing were carried out by F. Hardy, O. Bouchez, and F. Plume. We thank OWSF for their help in finding declining stands, for providing information about biotic attacks, and for providing the picture in Fig. 1. We thank the Seed Production Center for information about mast events and H. Titeux for his help in describing soil profiles and collecting soil samples. We thank N. Bréda for her advice on the sapwood observations and the definition of a growth crisis. We also thank RMI for providing us with climate data. Finally, we warmly thank the agents of Département de la Nature et des Forêts (DNF) for their collaboration. This work was supported by the Walloon Region (DGARNE/DNF) through the framework programs on forest research 2014–2019. The authors declare that they have no conflicts of interest.

References

Allen, C.D., Breshears, D.D., and McDowell, N.G. 2015. On underestimation of global vulnerability to tree mortality and forest die-off from hotter drought in the Anthropocene. Ecosphere, **6**: 129. doi:10.1890/ES15-00203.1.

Anderegg, W.R.L., Berry, J.A., and Field, C.B. 2012. Linking definitions, mechanisms, and modeling of drought-induced tree death. Trends Plant Sci. **17**(12): 693–700. doi:10.1016/j.tplants.2012.09.006. PMID:23099222.

Andersson, M., Milberg, P., and Bergman, K.O. 2011. Low pre-death growth rates of oak (*Quercus robur* L.) — is oak death a long-term process induced by dry years? Ann. For. Sci. **68**(1): 159–168. doi:10.1007/s13595-011-0017-y.

André, P., and Laudelout, H. 1992. Le dépérissement du chêne. Etat de la question et bibliographie. For. Wallonne, **14**: 16–19.

Anfodillo, T., Petit, G., Sterck, F., Lechthaler, S., and Olson, M.E. 2016. Allometric trajectories and "stress": a quantitative approach. Front. Plant Sci. **7**: 1681. PMID:27881990.

Barbaroux, C., and Bréda, N. 2002. Contrasting distribution and seasonal dynamics of carbohydrate reserves in stem wood of adult ring-porous sessile oak and diffuse-porous beech trees. Tree Physiol. **22**(17): 1201–1210. doi:10.1093/treephys/22.17.1201. PMID:12464573.

Becker, M., and Levy, G. 1990. Le point sur l'écologie comparée du chêne sessile et du chêne pédonculé. Rev. For. Fr. **42**(2): 148–154.

Bréda, N., and Badeau, V. 2008. Forest tree responses to extreme drought and some biotic events: towards a selection according to hazard tolerance? C. R. Geosci. **340**(9–10): 651–662. doi:10.1016/j.crte.2008.08.003.

Bréda, N., and Peiffer, M. 2014. Vulnerability to forest decline in a context of climate changes: new prospects about an old question in forest ecology. Ann. For. Sci. **71**(6): 627–631. doi:10.1007/s13595-014-0411-3.

Cailleret, M., Jansen, S., Robert, E.M.R., Desoto, L., Aakala, T., Antos, J.A., et al. 2017. A synthesis of radial growth patterns preceding tree mortality. Glob. Change Biol. **23**(4): 1675–1690. doi:10.1111/gcb.13535.

Bréda, N., Huc, R., Granier, A., and Dreyer, E. 2006. Temperate forest trees and stands under severe drought: a review of ecophysiological responses, adaptation processes and long-term consequences. Ann. For. Sci. **63**(6): 625–644. doi:10.1051/forest:2006042.

Camarero, J.J., Gazol, A., Sangüesa-Barreda, G., Oliva, J., and Vicente-Serrano, S.M. 2015. To die or not to die: early warnings of tree dieback in response to a severe drought. J. Ecol. **103**(1): 44–57. doi:10.1111/1365-2745.12295.

De Micco, V., Balzano, A., Wheeler, E.A., and Baas, P. 2016. Tyloses and gums: a review of structure, function and occurrence of vessel occlusion. IAWA J. **37**(2): 186–205. doi:10.1163/22941932-20160130.

Delatour, C. 1983. Les dépérissements des chênes en Europe. Rev. For. Fr. **265**(4): 265–282.

Denman, S., Barrett, G., Kirk, S.A., McDonald, J.E., and Coetzee, M.P.A. 2017. Identification of *Armillaria* species on declined oak in Britain: implications for oak health. For.: Int. J. For. Res. **90**(1): 148–161. doi:10.1093/forestry/cpw054.

Eichhorn, J., Roskams, P., Potočić, N., Timmermann, V., Ferretti, M., Mues, V., et al. 2016. Part IV. Visual assessment of crown condition and damaging agents. *In* Manual on methods and criteria for harmonized sampling, assessment, monitoring and analysis of the effects of air pollution on forests. *Edited by* UNECE ICP Forests Programme Co-ordinating Centre. Thünen Institute of Forest Ecosystems, Eberswalde, Germany.

Ellmore, G.S., and Ewers, F.W. 1986. Fluid flow in the outermost xylem increment of a ring-porous tree, *Ulmus americana*. Am. J. Bot. **73**(12): 1771–1774. doi:10.1002/j.1537-2197.1986.tb09709.x.

Fernández-Martínez, M., Belmonte, J., and Maria Espelta, J. 2012. Masting in oaks: disentangling the effect of flowering phenology, airborne pollen load and drought. Acta Oecol. **43**(Suppl. C): 51–59.

Focant, A., and Malaisse, F. 2001. Dépérissement du chêne en Wallonie : état de la question. For. Wallonne, **49–50**: 17–35.

Galoux, D., and Dutrecq, A. 1990. Le dépérissement du Chêne. A propos des mortalités récentes des chênes pédonculé et sessile en Hesbaye, en Condroz et en Ardenne convinoise. For. Wallonne, **7**: 3–8.

Granier, A., Anfodillo, T., Sabatti, M., Cochard, H., Dreyer, E., Tomasi, M., et al. 1994. Axial and radial water flow in the trunks of oak trees: a quantitative and qualitative analysis. Tree Physiol. **14**(12): 1383–1396. doi:10.1093/treephys/14.12.1383. PMID:14967611.

Grissino-Mayer, H.D. 2001. Evaluating crossdating accuracy: a manual and tutorial for the computer program COFECHA. Tree-Ring Res. **57**(2): 205–221.

Haavik, L.J., Billings, S.A., Guldin, J.M., and Stephen, F.M. 2015. Emergent insects, pathogens and drought shape changing patterns in oak decline in North America and Europe. For. Ecol. Manage. **354**: 190–205. doi:10.1016/j.foreco.2015.06.019.

Hargreaves, G.H., and Samani, Z.A. 1985. Reference crop evapotranspiration from temperature. Appl. Eng. Agric. **1**(2): 96–99.

Hartmann, G., and Blank, R. 1992. Winter frost, insect defoliation and *Agrilus biguttatus* Fabr. as causal factors of oak decline in northern Germany. Forst Holz, **47**: 443–452.

Hartmann, H., Moura, C.F., Anderegg, W.R.L., Ruehr, N.K., Salmon, Y., Allen, C.D., et al. 2018. Research frontiers for improving our understanding of drought-induced tree and forest mortality. New Phytol. **218**: 15–28. doi:10.1111/nph.15048. PMID:29488280.

Hendriks, K., Klap, J.M., de Jong, E., van Leeuwen, E.P., and de Vries, W. 1997. Calculation of natural stress factors. *In* Ten years of monitoring forest condition in Europe. Studies on temporal development, spatial distribution and impacts of natural and anthropogenic stress factors. *Edited by* C. Müller-Edzards and W. de Vries. United Nations Economic Commission for Europe (ECE), Geneva, and European Commission (EC), Brussels. pp. 225–239.

Jonard, M., Legout, A., Nicolas, M., Dambrine, E., Nys, C., Ulrich, E., et al. 2012. Deterioration of Norway spruce vitality despite a sharp decline in acid deposition: a long-term integrated perspective. Glob. Change Biol. **18**(2): 711–725. doi:10.1111/j.1365-2486.2011.02550.x.

Klap, J.M., de Vries, W., Hendriks, C.M.A., Oude Voshaar, J.H., Reinds, G.J., van Leeuwen, E.P., and Erisman, J.W. 1997. Assessment of the possibilities to derive relationships between stress factors and forest condition for Europe. Rep. 149. DLO Winand Staring Centre for Integrated Land, Soil and Water Research.

Kreuzwieser, J., and Gessler, A. 2010. Global climate change and tree nutrition: influence of water availability. Tree Physiol. **30**(9): 1221–1234. doi:10.1093/treephys/tpq055. PMID:20581013.

Landman, G. 1994. Concepts, définitions et caractéristiques générales des dépérissements forestiers. Rev. For. Fr. **46**(5 NS): 405–415.

Lebourgeois, F., Cousseau, G., and Ducos, Y. 2004. Climate-tree-growth relationships of *Quercus petraea* Mill. stand in the Forest of Bercé ("Futaie des Clos", Sarthe, France). Ann. For. Sci. **61**(4): 361–372.

Losseau, J., Jonard, M., Titeux, H., and Vincke, C. 2018. Les dépérissements récents du chêne pédonculé en Ardenne: une longue histoire? For. Nat. **147**: 35–47.

Lucassen, E., Van den Berg, L., Aben, R., Smolder, F., Roelofs, J., and Bobbink, R. 2014. Bodemverzuring en achteruitgang zomereik. Landschap, **4**: 185–193.

Manion, P.D. 1991. Tree disease concepts. Prentice-Hall, Englewood Cliffs, N.J.

Marçais, B., and Desprez-Loustau, M.-L. 2014. European oak powdery mildew: impact on trees, effects of environmental factors, and potential effects of climate change. Ann. For. Sci. **71**(6): 633–642. doi:10.1007/s13595-012-0252-x.

McDowell, N.G. 2011. Mechanisms linking drought, hydraulics, carbon metabolism, and vegetation mortality. Plant Physiol. **155**(3): 1051–1059. doi:10.1104/pp.110.170704. PMID:21239620.

Mérian, P., and Lebourgeois, F. 2011. Consequences of decreasing the number of cored trees per plot on chronology statistics and climate–growth relationships: a multispecies analysis in a temperate climate. Can. J. For. Res. **41**(12): 2413–2422. doi:10.1139/x11-149.

Miao, S., Zou, C.B., and Breshears, D.D. 2009. Vegetation responses to extreme hydrological events: sequence matters. Am. Nat. **173**(1): 113–118. doi:10.1086/593307. PMID:19061420.

Niinemets, Ü. 2010. Responses of forest trees to single and multiple environmental stresses from seedlings to mature plants: past stress history, stress interactions, tolerance and acclimation. For. Ecol. Manage. **260**(10): 1623–1639. doi:10.1016/j.foreco.2010.07.054.

Piraux, C., Ponette, Q., and Vincke, C. 2016. Base de données "Aléas" Recenser l'historique des aléas climatiques et biotiques en forêt wallonne comme outil pour la gestion adaptative. For. Nat. **141**: 40–45.

R Core Team. 2013. R: a language and environment for statistical computing. R Foundation for Statistical Computing, Vienna, Austria.

Rodríguez-Calcerrada, J., Sancho-Knapik, D., Martin-StPaul, N.K., Limousin, J.-M., McDowell, N.G., and Gil-Pelegrín, E. 2017. Drought-induced oak decline — factors involved, physiological dysfunctions, and potential attenuation by forestry practices. *In* Oaks physiological ecology. Exploring the functional diversity of genus *Quercus* L. *Edited by* E. Gil-Pelegrín, J.J. Peguero-Pina, and D. Sancho-Knapik. Springer, Cham, Switzerland. pp. 419–451.

Rouault, G., Candau, J.-N., Lieutier, F., Nageleisen, L.-M., Martin, J.-C., and Warzée, N. 2006. Effects of drought and heat on forest insect populations in relation to the 2003 drought in Western Europe. Ann. For. Sci. **63**(6): 613–624. doi:10.1051/forest:2006044.

Rubtsov, V.V. 1996. Influence of repeated defoliations by insects on wood increment in common oak (*Quercus robur* L.). Ann. For. Sci. **53**: 407–412. doi:10.1051/forest:19960223.

Sala, A., Woodruff, D.R., and Meinzer, F.C. 2012. Carbon dynamics in trees: feast or famine? Tree Physiol. **32**(6): 764–775. doi:10.1093/treephys/tpr143. PMID:22302370.

Sass-Klaassen, U., Sabajo, C.R., and den Ouden, J. 2011. Vessel formation in relation to leaf phenology in pedunculate oak and European ash. Dendrochronologia, **29**(3): 171–175. doi:10.1016/j.dendro.2011.01.002.

Schweingruber, F.H. 1996. Tree rings and environment: dendroecology. Swiss Federal Institute for Forest, Snow and Landscape Research, and Paul Haupt Verlag, Bern.

Sonesson, K., and Drobyshev, I. 2010. Recent advances on oak decline in southern Sweden. Ecol. Bull. **53**: 197–207.

Thomas, F.M., Blank, R., and Hartmann, G. 2002. Abiotic and biotic factors and their interactions as causes of oak decline in Central Europe. For. Pathol. **32**(4–5): 277–307. doi:10.1046/j.1439-0329.2002.00291.x.

Van der Perre, R., Bythell, S., Bogaert, P., Claessens, H., Ridremont, F., Tricot, C., et al. 2015. La carte bioclimatique de Wallonie : un nouveau découpage écologique du territoire pour le choix des essences forestières. For. Nat. **135**: 47–58.

Vicente-Serrano, S.M., Beguería, S., and López-Moreno, J.I. 2010. A multiscalar drought index sensitive to global warming: the standardized precipitation evapotranspiration index. J. Clim. **23**(7): 1696–1718. doi:10.1175/2009JCLI2909.1.

Villemant, C., and Fraval, A. 1998. Lymantria dispar en Europe et en Afrique du Nord. *In* Protection intégrée des forêts à *Quercus* spp. *Edited by* INRA. Courrier de l'INRA, Salé (Maroc).

Voltas, J., Camarero, J.J., Carulla, D., Aguilera, M., Ortiz, A., and Ferrio, J.P. 2013. A retrospective, dual-isotope approach reveals individual predispositions to winter-drought induced tree dieback in the southernmost distribution limit of Scots pine. Plant, Cell Environ. **36**(8): 1435–1448. doi:10.1111/pce.12072. PMID:23346991.

Walloon Forest Health Observatory (OWSF). 2014. La lettre de l'OWSF numéro 2 : l'acualité sanitaire de nos forêts wallonnes en 2014 [online]. Available from http://owsf.environnement.wallonie.be/fr/16-03-2015-la-lettre-de-l-owsf-numero-2.html?IDC=5792&IDD=4731.

Zadworny, M., Jagodziński, A.M., Łakomy, P., Mucha, J., Oleksyn, J., Rodríguez-Calcerrada, J., and Ufnalski, K. 2019. Regeneration origin affects radial growth patterns preceding oak decline and death — insights from tree-ring $\delta^{13}C$ and $\delta^{18}O$. Agric. For. Meteorol. **278**: 107685. doi:10.1016/j.agrformet.2019.107685.